Child's Nervous System (2019) 35:2399–2403
https://doi.org/10.1007/s00381-019-04289-8

TECHNICAL NOTES

Quantitative color-coded digital subtraction neuroangiography for pediatric arteriovenous shunting lesions

Grace M. Y. Ma[1] · Adam A. Dmytriw[1,2] · Premal A. Patel[3,4] · Nicholas Shkumat[1] · Timo Krings[2] · Manohar M. Shroff[1] · Prakash Muthusami[1]

Received: 27 May 2019 / Accepted: 30 June 2019 / Published online: 6 July 2019

Abstract

Background Several complex pediatric neurovascular conditions are amenable to endovascular treatment. Given the unique anatomical and physiological challenges in children, there is an ongoing need for tools and techniques that provide accurate information for treatment planning, while minimizing exposure to ionizing radiation and contrast. This is more so for neonates and infants with high-flow arteriovenous (AV) shunts that are challenging to assess using conventional techniques.

Objective In this brief report, we describe, through representative cases, the potential role of quantitative color-coded digital subtraction angiography (qDSA) in neuroendovascular procedures in children with high-flow AV shunting lesions.

Methods Images were obtained using an ArtisQ biplane system (Siemens Healthineers, Erlangen, Germany). Post-processing was performed at a dedicated workstation (Syngo, Siemens) using the iFlow module to generate color-coded maps of individual digital subtraction angiography runs.

Conclusion Color-coded qDSA provides real-time quantitative information in high-flow AV shunting neurovascular lesions. This can potentially help direct treatment choices, optimize endovascular treatment protocols, monitor outcomes, and determine treatment end points.

Keywords Arteriovenous · Quantitative · Digital subtraction angiography · iFlow · Children

Introduction

Endovascular treatments of neurovascular pathology in children pose unique challenges arising from patient size, weight, and hemodynamics [3]. There has been significant interest in the pediatric literature regarding radiation and contrast dose limitations during these procedures [2, 5, 7, 9, 10]. Multimodal investigations are commonly performed with the aim of reducing radiation exposure during angiography to obtain information needed for treatment planning and follow-up.

In this report, the potential for color-coded quantitative digital subtraction angiography (qDSA) to provide unique information in high-flow arteriovenous (AV) shunting lesions is described. Syngo iFlow (Siemens Healthineers, Erlangen, Germany), a commercially available post-processing software, allows visualization of a complete digital subtraction angiography (DSA) run in a single color-coded image, which is a map of the contrast flow dynamics through the run. It provides a time curve of contrast intensity for any pixel or region of interest (ROI). Through this, an objective assessment of inflow and outflow of contrast is possible; this allows evaluation of blood flow parameters such as time to peak (TTP) or area under the curve (AUC) without added radiation or contrast.

✉ Grace M. Y. Ma
gracemy.ma@gmail.com

1 Image Guided Therapy, Department of Diagnostic Imaging, Department of Medical Imaging, Hospital for Sick Children, University of Toronto, 555 University Ave, Toronto, ON M5S, Canada

2 Division of Neuroradiology, Joint Department of Medical Imaging, Toronto Western Hospital, University Health Network, University of Toronto, Toronto, Ontario, Canada

3 Wellcome / EPSRC Centre for Interventional and Surgical Sciences (WEISS), University College London, Bloomsbury, London WC1E 6BT, UK

4 Radiology Department, Great Ormond Street Hospital for Children, London, UK

Methods

Images were obtained using an ArtisQ biplane system (Siemens Healthineers, Erlangen, Germany) at 3–6 frames per second by hand injection of 2–5 mL of Omnipaque 300. Post-processing was performed at a dedicated workstation (Syngo, Siemens) using the iFlow module to generate color-coded maps of individual DSA runs. Manual ROIs were defined on arterial feeders and venous outflow, which resulted in generation of TTP values and time-intensity curves.

Illustrative cases

Case 1 (pial arteriovenous fistula in a neonate)

A 3-month-old infant was referred for embolization of a prenatally diagnosed pial arteriovenous fistula (AVF). MRI and DSA showed a large venous pouch secondary to a high-flow direct shunt from the rolandic left middle cerebral artery (MCA) branch, through superficial cortical veins, into the superior sagittal sinus and sigmoid sinus (Fig. 1a), resulting in hemispheric venous congestion. Endovascular embolization was performed using undiluted *n*-butyl cyanoacrylate (NBCA) opacified with tantalum until complete shunt exclusion (Fig. 1b). Improvement of intra-cerebral hemodynamics can be posited from qDSA-derived TTP in the MCA branch (3.00 s pre-embolization vs. 5.96 s post-embolization), in the sigmoid sinus (4.50 s pre-embolization vs. 11.76 s post-embolization), and from the parenchymal ROIs (circle in Fig. 1a and b), which showed correction of the slow, prolonged rise of the time-intensity curve due to pre-interventional steal phenomenon. More flow throughout the brain parenchyma post embolization is readily seen on the color map (Fig. 1b). At last follow-up in clinic, 20 months following embolization, the child is healthy and developmentally and neurocognitively age appropriate.

Case 2 (assessing AVM treatment response)

An 11-year-old boy presented with acute onset of headache, emesis, left hemiplegia, and decreased level of consciousness. CT and DSA showed right intraventricular hemorrhage from a frontoparietal arteriovenous malformation (AVM) that was supplied by MCA branches. Rapid venous drainage into the internal cerebral/Galenic system (TTP 4.85 s) and relatively slower superficial venous drainage through dilated veins into the superior sagittal sinus (TTP 5.83 s) were identified (Fig. 2a). DSA performed 1-year post Gamma-Knife treatment due to increasing headaches showed expected reduction in nidus size, deep venous outflow stenosis, and redirection of outflow into cortical veins, identified from alteration of blood flow on the qDSA-generated time-intensity curves (Fig. 2b). This redistribution to the superficial venous system, evidenced by the relative AUCs (superficial vs. deep), increases diagnostic confidence for the non-significance of the deep venous stenosis. This patient was followed conservatively, has remained asymptomatic, and showed continuing reduction in

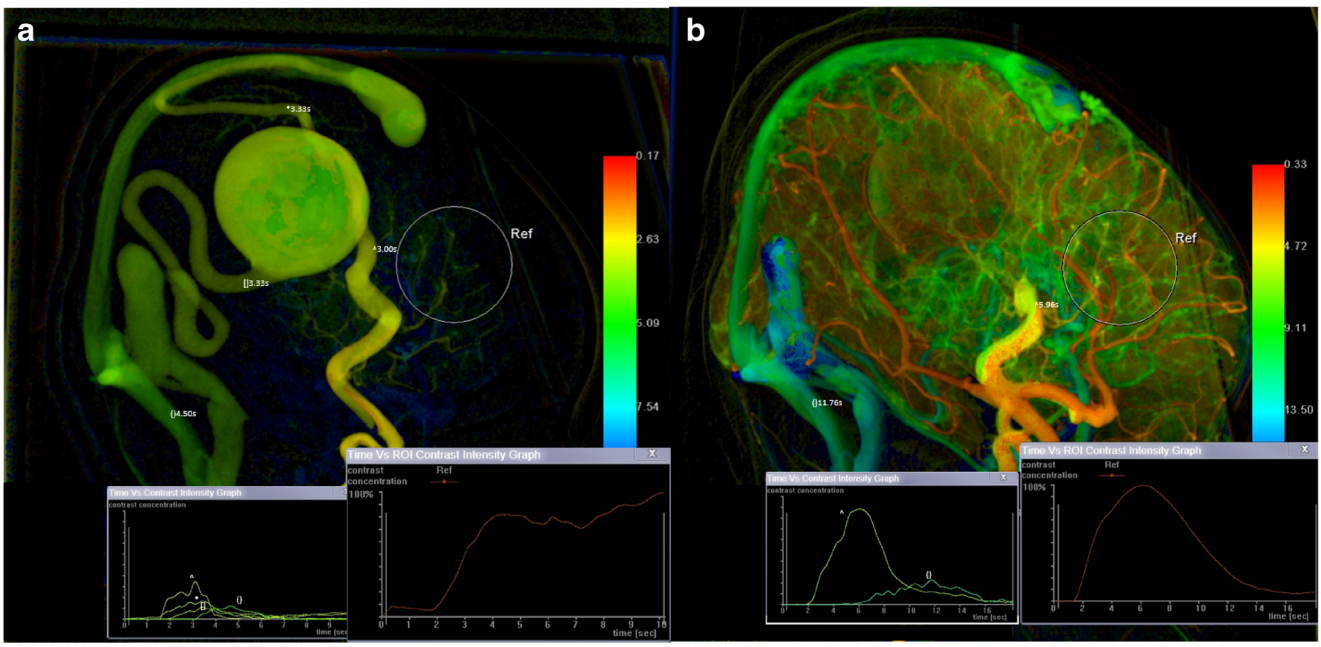

Fig. 1 Lateral **a** pre- and **b** post-embolization qDSA images of a middle cerebral pial AVF in an infant. **a** Time-intensity curves show rapid flow through the superficial cortical veins, quantified from time to peak (TTP) values (arterial 3.00 s, venous 3.33 s). **b** The venous pouch and draining veins are no longer visualized post-embolization. Time-intensity curves from frontal parenchymal ROIs show correction of the slow prolonged rise due to vascular steal

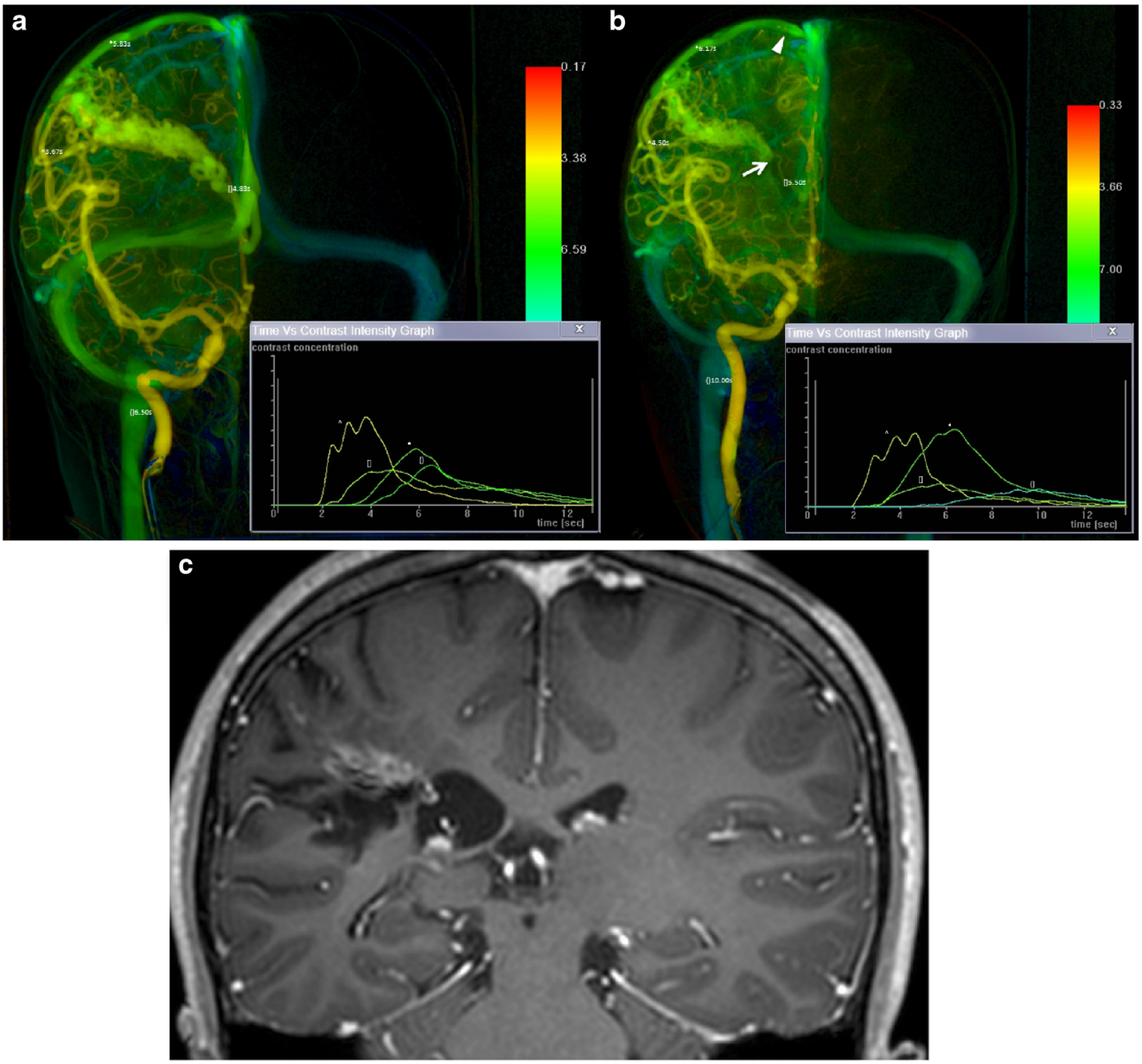

Fig. 2 Frontal qDSA images of a right frontoparietal AVM **a** before and **b** 1 year following Gamma-Knife treatment. Time-intensity curves are generated from pixels in the feeding artery and draining veins. **a** Initial hemodynamics shows a rapid shunt with venous outflow distributed between deep and superficial veins, as seen from similar AUC of time-intensity curves in superficial and deep veins. **b** Follow-up DSA showed deep venous outflow stenosis (arrow), with superficial venous redirection (arrowhead). This altered hemodynamic can be seen as an increased AUC of the curve generated from the superficial vein. Reduced shunting is suggested from an increase in arterial TTP (3.67 s before treatment vs. 4.50 s following treatment) and TTP in the internal jugular vein (6.50 s before treatment vs. 10.00 s following treatment). **c** Coronal reformat from follow-up post-gadolinium 3D-T1 MRI performed 9 months following the last angiogram showed further interval reduction in the nidus size, as well as regression in size of arterial feeders and draining veins

size of nidus and draining veins on MRI performed 9 months following the last angiogram (Fig. 2c).

Case 3 (scalp AVF pre-surgical embolization)

A 5-year-old boy presented with a growing, pulsatile posterior scalp lesion with multiple episodes of bleeding. MRI and DSA showed a left scalp AVF with supply from bilateral occipital arteries and superficial temporal arteries (Fig. 3a). Following embolization of multiple feeders with NBCA, qDSA demonstrated complete shunt exclusion with uncompromised cerebrovascular circulation (Fig. 3b). The lesion was surgically excised the following day. At last clinic follow-up 10 months after surgery, he is doing well, with no clinical recurrence. Repeat imaging is planned at 1 year.

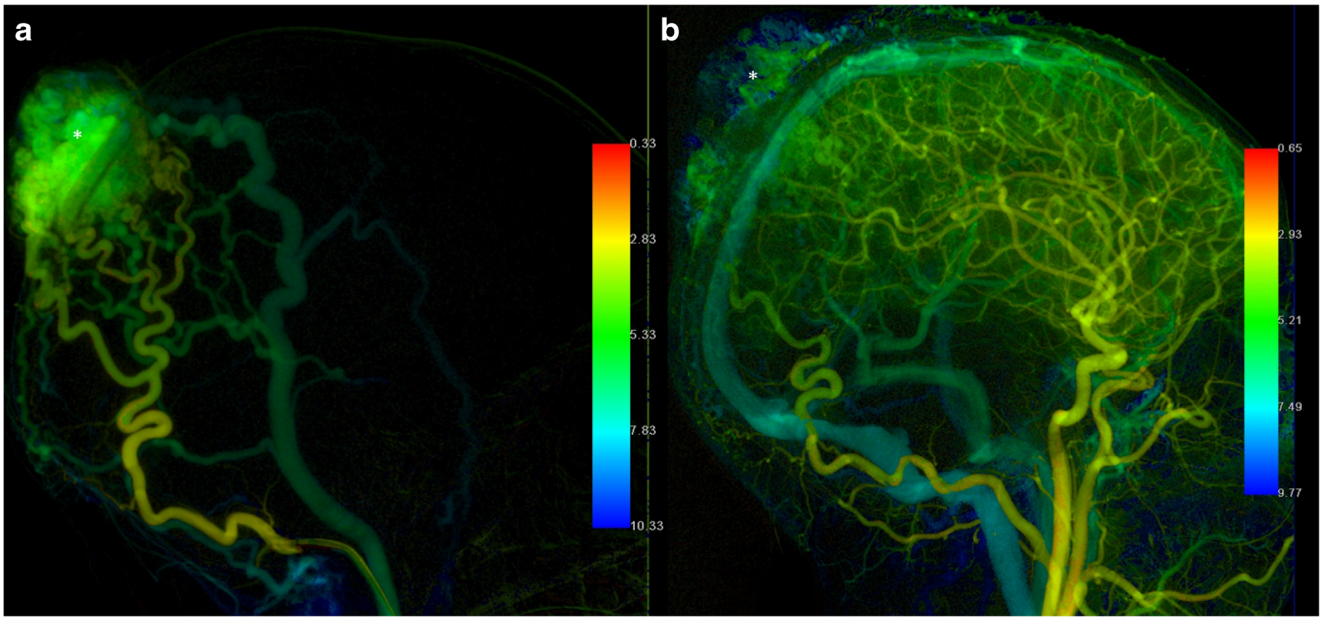

Fig. 3 Lateral qDSA images of a posterior scalp AVF near the vertex (*). **a** Relatively rapid shunting via dilated venous lakes can be appreciated on the pre-embolization qDSA image. **b** On post-embolization images, although the venous lakes still stain on angiography, the venous shunting can be seen to have disappeared, which is determined as an adequate end point for pre-surgical devascularization

Case 4 (vertebral–venous fistula follow-up)

A 9-year-old girl presented with a vertebral–venous fistula involving the V1 segment of the left vertebral artery with epidural reflux and resultant venous congestion (Fig. 4a). Near-complete obliteration of the large post-fistulous venous sac was achieved with multiple coils and Amplatzer vascular plug 4 (Abbott, Abbott Park, IL). A 6-month

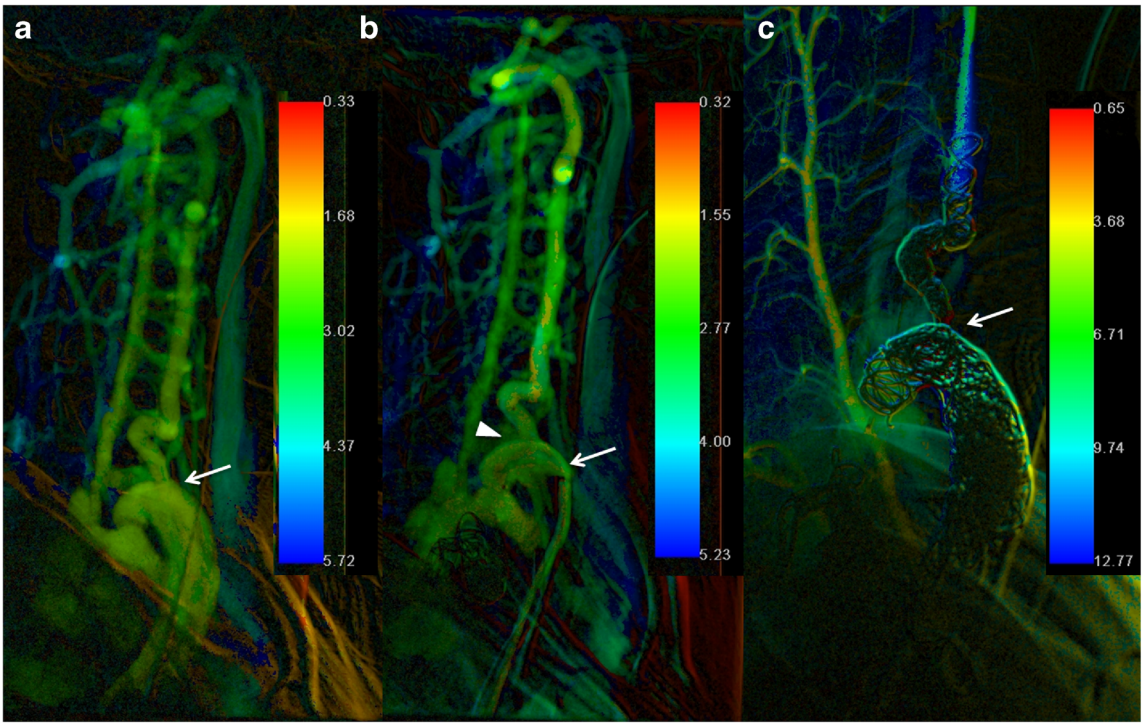

Fig. 4 Lateral qDSA images of a vertebral–venous fistula from the V1 segment of the left vertebral artery (arrow). **a** Epidural venous congestion is seen pre-embolization, which largely resolved following embolization of the large venous sac. **b** Recurrence after 6 months, with qDSA demonstrating the fistulous point (arrowhead) and venous congestion comparable to prior. **c** Complete cure after endovascular coil sacrifice of the left vertebral artery (arrow). Note that the extent of venous congestion can be assessed qualitatively on the composite qDSA images

follow-up angiogram showed recurrent shunting (Fig. 4b), which was treated with endovascular coil ligation of the vertebral artery across the neck of the fistula (Fig. 4c).

Discussion

The assessment of hemodynamics plays an important role in evaluating high-flow AV shunting lesions in children and their endovascular treatment. Color-coded qDSA (e.g., Syngo iFlow, Siemens; and AngioViz, GE Healthcare) provides qualitative and quantitative information on flow characteristics which are otherwise assessed only by visual inspection of the DSA run. This technique does not require additional radiation or contrast and can be applied on any DSA run without the need for a dedicated acquisition protocol. The basic premise is to integrate information from a contrast bolused DSA run to generate a map containing TTP information within each pixel. This allows evaluation of arterial inflow, aberrant AV connections, and venous outflow of an AV shunting lesion on the same image. Flow curves (time- vs. contrast-intensity) can be generated for any pixel or ROI of any shape to allow direct quantitative comparison of flow characteristics. This can be useful for several situations; for instance, before and after embolization (Figs. 1 and 3), follow-up evaluation of flow through AVMs (Figs. 2 and 4), and to determine treatment end points (Figs. 3 and 4). Flow curves can be used to quantify vascular shunting through the lesion (from the AUC), and arterial steal from normal brain (Fig. 1). Transit times measured with qDSA were previously shown to correlate well with cerebral AVM flow measurements on quantitative MRI, allowing for real-time quantification of flow during endovascular treatment [8].

Other applications for qDSA have been described. Cattaneo et al. reported the use of qDSA to assess intra-aneurysmal flow during treatment with flow-diverting devices [1]. Kondapavulur et al. described using qDSA to quantify the distribution of super-selective intra-arterial chemotherapy delivery to ocular target tissues in retinoblastoma [6]. qDSA has also been used to evaluate/grade degrees of arterial stenosis in adults [4]. Although there is not enough data in literature to make sense of individual TTP and AUC values, cases can be used as their own controls to assist in clinical decisions during endovascular procedures.

In conclusion, color-coded qDSA provides real-time quantitative information in high-flow AV shunting neurovascular lesions. This can potentially help direct treatment choices, optimize endovascular treatment protocols, monitor outcomes, and determine treatment end points.

Funding No funding was received for this study.

Compliance with ethical standards

Conflict of interest On behalf of all authors, the corresponding author states that there is no conflict of interest.

Ethical approval The study was approved by the Institutional Research Ethics Board (REB)

References

1. Cattaneo GFM, Ding A, Jost T, Ley D, Muhl-Bennighaus R, Yilmaz U, Korner H, Reith W, Simgen A (2017) In vitro, contrast agent-based evaluation of the influence of flow diverter size and position on intra-aneurysmal flow dynamics using syngo iFlow. NRJ 59:1275–1283
2. Chida K, Ohno T, Kakizaki S, Takegawa M, Yuuki H, Nakada M, Takahashi S, Zuguchi M (2010) Radiation dose to the pediatric cardiac catheterization and intervention patient. AJR 195:1175–1179
3. Ganjoo P (2018) Challenges in paediatric neurosurgery. J Neuroanaesthesiol Crit Care 04:S19–S23
4. Ghibes P, Partovi S, Grozinger G, Martirosian P, Schick F, Nikolaou K, Ketelsen D, Syha R, Grosse U (2018) Reliability and accuracy of peri-interventional stenosis grading in peripheral artery disease using color-coded quantitative fluoroscopy: a phantom study comparing a clinical and scientific postprocessing software. Biomed Res Int 2018:6180138
5. Kim S, Yoshizumi TT, Frush DP, Toncheva G, Yin FF (2010) Radiation dose from cone beam CT in a pediatric phantom: risk estimation of cancer incidence. AJR 194:186–190
6. Kondapavulur S, Cooke DL, Kao A, Amans MR, Alexander M, Darflinger R, Dowd CF, Higashida RT, Damato B, Halbach VV, Matthay KK, Hetts SW (2018) Estimation of intra-arterial chemotherapy distribution to the retina in pediatric retinoblastoma patients using quantitative digital subtraction angiography. Interv Neuroradiol 24:214–219
7. Orbach DB, Stamoulis C, Strauss KJ, Manchester J, Smith ER, Scott RM, Lin N (2014) Neurointerventions in children: radiation exposure and its import. AJNR 35:650–656
8. Shakur SF, Brunozzi D, Hussein AE, Linninger A, Hsu CY, Charbel FT, Alaraj A (2018) Validation of cerebral arteriovenous malformation hemodynamics assessed by DSA using quantitative magnetic resonance angiography: preliminary study. J Neurointerv Surg 10:156–161
9. Shkumat NA, Shroff MM, Muthusami P (2018) Radiation dosimetry of 3D rotational neuroangiography and 2D-DSA in children. AJNR 39:727–733
10. Thierry-Chef I, Simon SL, Miller DL (2006) Radiation dose and cancer risk among pediatric patients undergoing interventional neuroradiology procedures. Pediatr Radiol 36(Suppl 2):159–162